Journal of Energy Storage 44 (2021) 103309

Contents lists available at ScienceDirect

Journal of Energy Storage

journal homepage: www.elsevier.com/locate/est

A voltage dynamic-based state of charge estimation method for batteries storage systems

Marco Mussi [a], Luigi Pellegrino [b], Marcello Restelli [a], Francesco Trovò [a,*]

[a] Politecnico di Milano, Piazza L. da Vinci, 32, Milan, Italy
[b] Ricerca Sistema Energetico (RSE) S.p.A., Via R. Rubattino, 54, Milan, Italy

ARTICLE INFO

Keywords:
State of charge estimation
Lithium-ion batteries
Online model

ABSTRACT

In recent years, the use of Lithium-ion batteries in smart power systems and hybrid/electric vehicles has become increasingly popular since they provide a flexible and cost-effective way to store and deliver power. Their full integration into more complex systems requires an accurate estimate of the energy a battery is currently storing, a.k.a. State of Charge (SoC). However, the standard techniques present in the literature provide an accurate estimation of the SoC only having a priori knowledge about the battery. Moreover, their accuracy degrades if the battery working conditions (*e.g.,* external temperature) are variable over time, or battery measurements necessary for the SoC estimation are affected by offset or gain biases. To overcome these limitations, this paper proposes a novel data-driven optimization based methodology for battery SoC estimation, namely VDB-SE. The proposed methodology provides accurate SoC estimations without knowing battery model parameters, such as capacity and internal resistance, whose characterization would require complex and long laboratory tests. Experimental verification and comparisons demonstrate that VDB-SE performance are comparable to the state-of-the-art algorithms over a wide range of working conditions. Indeed, the difference in terms of performance is smaller than 0.2%. Moreover, experimental results showed that on a real energy storage system the proposed method provides a SoC estimation with an error of less than 2.1%.

1. Introduction

In recent years, the use of batteries in a wide range of energy-management systems has become a key element to be handled by energy managers [1]. For instance, according to the International Renewable Energy Agency [2], focusing only on battery storage in stationary applications, they are expected to store a total amount of 235 GW in 2030, which rivals the one provided today by pumped-hydro storage. Indeed, lithium-ion batteries have become more efficient and less unwieldy, allowing them to be used in both self-consumption systems to compensate for the excesses and abundance of energy production in smart grid architectures, as well as in electric and hybrid vehicles [3], where they can deliver power in a prompt and fast way without adding too much weight to the vehicle. A critical issue with these applications is that they require accurate, real-time estimation of the State-of-Charge (SoC), defined as the ratio between the charge remaining in the battery and the maximum charge accumulated when the battery is fully charged. Indeed, SoC estimation is a crucial factor for efficient battery management since energy consumption policies are commonly based on the remaining charge and assume to have a reliable prediction of energy consumption given a specific load. However, unlike other electric measurements, there is no physical sensor to measure a battery SoC, and, therefore, it should be computed from other measurements coming from the battery, *e.g.,* current and voltage. This fact suggests using data-driven methods to model the SoC behaviour and predict its future values given a power consumption profile. Even if battery discharge models can be built using laboratory tests at the beginning of the battery life, they might provide unreliable predictions caused by the variation of the working conditions over time, *e.g.,* external temperature changes and battery ageing, and due to the fact that the physical measurements have small biases, *e.g.,* the measured current has a constant offset w.r.t. the real one [4].

In scientific literature, three different approaches for SoC estimation have been considered: physical-based, black-box, and model-based ones. None of the currently available approaches can handle the complex scenario of real-time SoC estimation without the knowledge of a priori information about the battery. More specifically, most physical-based models, such as Coulomb Counting [5], require frequent calibration of the estimator by disconnecting the battery from the power

* Corresponding author.
E-mail addresses: marco.mussi@polimi.it (M. Mussi), luigi.pellegrino@rse-web.it (L. Pellegrino), marcello.restelli@polimi.it (M. Restelli), francesco1.trovo@polimi.it (F. Trovò).

https://doi.org/10.1016/j.est.2021.103309
Received 17 June 2021; Received in revised form 9 September 2021; Accepted 23 September 2021
Available online 22 October 2021

system or performing a full charge, thus interrupting its functionality. Therefore, this approach is not feasible for those applications requiring no discontinuity of service, e.g., smart grids. Conversely, black-box techniques [6], even if they can adapt to new information coming from the system, to provide accurate predictions they require a large amount of data from the whole spectrum of the battery SoC (such as data coming from multiple full battery discharges) and from all the different working conditions the battery might encounter. Finally, the model-based methods [6] present so far in the literature require some *a priori* knowledge of the battery in use, e.g., the parameters of an equivalent model, and/or to set some hyper-parameter to provide accurate estimation performance, and, thus, they should be appropriately tuned for each new energy system. Even if the model-based approaches present in the literature do not provide a straightforward solution to the SoC estimation problem, they have pros over physical-based and black-box ones. Indeed, these solutions provide a parametric description of the battery, which can be used to manage the battery even more accurately.

Original contribution. The novel contribution provided by the current work are:

- the design of a novel model-based estimation procedure for the SoC, namely VDB-SE, which uses an electric battery model, the so-called Thevenin model [7,8], and the derivation of an optimization scheme for the SoC estimation of a generic battery based on the data-driven estimation of the model parameters.
- a method for battery SoC estimation which requires only the knowledge of the open circuit voltage function and the voltage and current measurements during the battery lifetime.
- an experimental campaign, based on simulation and field tests, showing that VDB-SE is robust to changes of the external temperature, battery ageing, and measurement uncertainty affecting real-world applications.

The paper is structured as follows: Section 2 reviews the currently available methods to estimate the SoC in Lithium-ion batteries; Section 3 describes the necessary background to introduce the presented method; Section 4 describes the proposed VDB-SE method in details; Section 5 provides a thorough experimental analysis of the proposed method; Section 6 draws some conclusions on the presented work and delineates the possible future works.

2. Related works

In what follows, the main related scientific works used for SoC estimation are reviewed. The section is divided into three paragraphs, corresponding to the three different ways to estimate the SoC of a battery: physical-based, black-box, and model-based. See Waag et al. [6], Zhang and Fan [9], Lipu et al. [10], and Qays et al. [11] for a complete review on this topic.

Physical-based approach. The most effective physical approach is the Coulomb Counting (CC), as described by Ng et al. [12]. This method estimates the SoC by knowing the initial SoC and using the inbound and outbound currents over time as an estimate for the SoC variation. CC shows good estimation performance over short periods but it accumulates error over time and it is not able to recover from an initial misspecification of the SoC. Therefore, it cannot be used in stationary applications, such as self-consumption, as it would require periodic recalibrations and, consequently, a temporary suspension of battery availability to obtain an accurate SoC estimate.

Black-box approach. The black-box category contains most of the data-driven approaches to solve the SoC estimation problem. The most common solution is to model the problem as a regression task and to use classic Machine Learning techniques to solve it. More specifically, the most used techniques are Artificial Neural Networks (ANN) [13–18], which provide results without having complete knowledge of the specific battery system, Support Vector Machines (SVM) [19–21], and Fuzzy Logic modelling [22,23]. The aforementioned solutions provide good empirical results thanks to the use of power profiles that explore all possible values for the SoC. This is because these techniques cannot generalize well into those regions of the input/output space that have not been explored well in the training set. However, having a large variety of power profiles is not common in practice, making this class of methods unsuitable for real-world applications.

Model-based approach. The model-based approach uses a mathematical model of the battery coupled with an algorithm to estimate the model parameters. Regarding the model, it has been shown by Hu et al. [24] and Einhorn et al. [25] that the first-order Thevenin RC equivalent model represents an interesting trade-off between the model complexity and an accurate representation of the system. For instance, Codeca et al. [26] starts from the knowledge of the parameters of this model to estimate the battery SoC in closed loop. Notice that despite them requiring additional information on the battery, such methods are regarded as state of the art for battery estimation [27].

As batteries may change some characteristics during their lifetime, the most suitable way to estimate the parameters turned out to be in the field of online learning. Indeed, the battery behaviour changes over time, requiring the model to follow the evolution of the storage system. The methodologies that have provided the best performance so far are those based on the Kalman Filter (KF) [28–30], which integrates new information as soon as it becomes available, thus adapting to the evolving behaviour of the battery. Plett [31,32] and Vasebi et al. [33] use an Extended Kalman Filter (EKF) to model, in a discrete way, the non-linear relationships that describe the dynamics of the components of the equivalent model. Xiong et al. [34], He et al. [35] and Xu et al. [36] extend this approach using Adaptive Extended Kalman Filter (AEKF) [37] for SoC estimation, self-adjusting its parameters, which in the previous case must be known. Sun et al. [38] and Wang et al. [39,40] propose a method based on the Unscented Kalman Filter (UKF), using a non-linear model for battery dynamics, and Cao et al. [41] and Li et al. [42] combine this approach with multiple parameter optimization methods. The main advantage of these approaches is that they work in a closed-loop, which allows reducing the error as soon as new measurements are available. Conversely, the main drawback is that they require prior knowledge of the battery system to properly initialize the model and setting properly the KF hyperparameters to quickly converge to an accurate estimate.

In addition to the categories mentioned above, there are also hybrid approaches that combine different methods, such as the one proposed by He et al. [43], using Artificial Neural Networks with Unscented Kalman Filters to reduce the noise in the SoC estimation. In this work, the UKF is used only to balance the high variability of the ANN, but the issues presented for the black-box approaches are still present.

In practice, Model-based methods and CC are the most widely used approaches. More specifically, the former has the intrinsic characteristic to follow the evolution of the system step by step, while the latter allows adopting this solution in multiple contexts due to the simplicity of the computational circuit it requires. Nonetheless, these methods are still limited in their usability (see Rivera-Barrera et al. [44] and Qays et al. [11] for a detailed discussion on their limitations).

3. Preliminaries

The State of Charge $SoC(t) \in [0,1]$ at time t is defined as follows:

$$SoC(t) := \frac{Q(t)}{Q_{\max}(t)}, \tag{1}$$

where $Q(t)$ is the actual capacity, and $Q_{\max}(t)$ the fully charged battery capacity at time t.[1]

[1] The selected measurement units are provided in Table 1. If no reference is provided, the quantity is dimensionless.

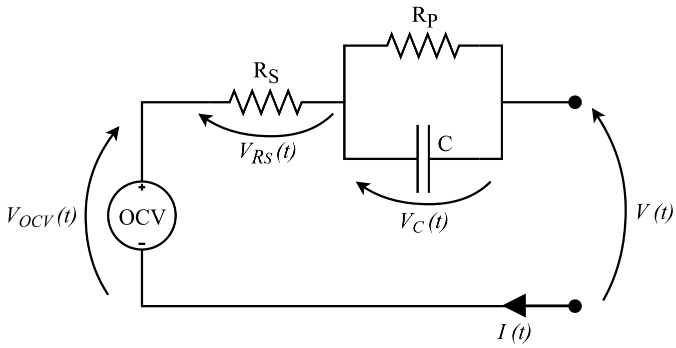

Fig. 1. Thevenin equivalent model of the battery.

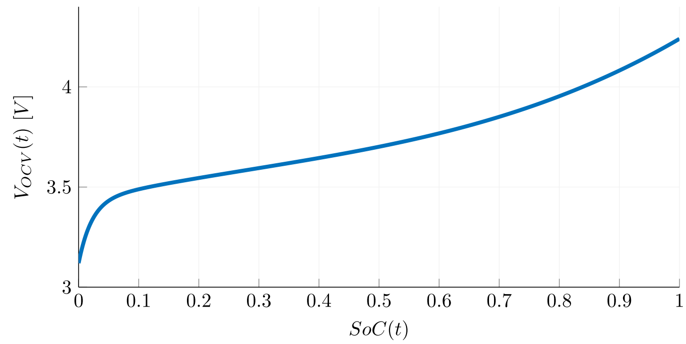

Fig. 2. Example of the nonlinear relationship $f(\cdot)$ between $SoC(t)$ and $V_{OCV}(t)$.

Table 1
Selected measurement units.

Quantity	Units
$Q(t)$, $Q_{\max}(t)$, Q_N	Ah
R_S, R_P	Ω
C	F
$I(t)$	A
$V(t)$, $V_{OCV}(t)$, $V_{R_S}(t)$, $V_C(t)$	V
t, Δt	s

Given that batteries capacity degrades over time, a definition of the State of Health (SoH) of the battery must be taken into account. Among the definitions available in literature, authors consider as most relevant for this problem the State of Health $SoH(t) \in [0,1]$ at time t is defined as:

$$SoH(t) := \frac{1}{1-p}\frac{Q_{\max}(t)}{Q_N} - \frac{p}{1-p}, \tag{2}$$

where p is the rate of the nominal capacity for which the battery cannot be used anymore for the selected application, and Q_N is the nominal capacity for the battery. For instance, for batteries used for automotive and self-consumption applications it is common to have a $SoH(t) = 0$ when the value of $Q_{\max}(t)$ is below the 80% of the nominal capacity, i.e., to use the value $p = 0.8$ [45].

Since the direct measurement of the SoC is not a viable option, it is common to use electrical models to characterize the battery behaviour and infer the SoC from it. It has been shown that the use of Thevenin's equivalent model [7,8], *i.e.,* a first-order electric RC model of the battery, shown in Fig. 1, is sufficient to model the dynamics of lithium-ion batteries. In this model, the battery is characterized by an internal impedance $R_S(SoC, SoH, T)$ in series with an RC group (consisting of a resistance $R_P(SoC, SoH, T)$ and a capacitance $C(SoC, SoH, T)$) and a voltage source, the Open Circuit Voltage $V_{OCV}(t)$.[2] Given this model, the SoC estimation problem is formalized as the estimation of the relationship between the current $I(t)$ and the voltage $V(t)$ with the SoC, given the curve that characterizes the relationship between the Open Circuit Voltage $V_{OCV}(t)$ and the State of Charge $SoC(t)$. More specifically, the SoC/Open Circuit Voltage function $f : SoC(t) \to V_{OCV}(t)$ predicts the $SoC(t)$ given $V_{OCV}(t)$ at a specific time t. An example of the above-mentioned relationship is presented in Fig. 2. Note that, given a battery model, this function $f(\cdot)$ regulating the dependence of $V_{OCV}(t)$ and $SoC(t)$ has been proven to be experimentally constant over time [46], therefore, it requires to be estimated only once for each battery. Commonly, the estimation is done by the battery producer; otherwise, it can be estimated as shown by [47].[3]

4. Proposed method

The approach proposed in this work, namely *Voltage Dynamic-Based State Estimation* (VDB-SE), aims at providing an estimate of the SoC, during the operational life of a battery given the current and voltage measurements. The proposed methodology exploits a discretization of the battery dynamics over time and uses it to optimize the parameters of Thevenin's battery model. Indeed, this work uses batches of data collected using the battery measurement instruments to retrieve the parameters of the equivalent Thevenin's battery model and minimizes the voltage reconstruction error using a non-linear optimization approach. Finally, thanks to the estimated model combined with the SoC/Open Circuit Voltage relationship $f(\cdot)$, it generates the SoC estimate.

The proposed model requires two time series, *i.e.,* the measurements of the battery current $I(t)$ and the voltage $V(t)$, over a finite time horizon $t \in \mathcal{T}$, and the function $f(\cdot)$ linking the SoC with the V_{OCV}.

As a preliminary to the description of the VDB-SE algorithm, in what follows, it is provided a formal derivation for the dynamics of $V(t)$ provided by Thevenin's equivalent model. Using Kirchhoff's laws on the model, the following relationship among the voltage values of a Lithium-ion battery can be inferred:

$$V_{OCV}(t) = V(t) + V_{R_S}(t) + V_C(t), \tag{3}$$

where $V_{R_S}(t)$ and $V_C(t)$ are the voltage over the resistance R_S and the RC group at time t, respectively, as shown in Fig. 1.

The dynamic evolution of the battery system over time comes from the derivation of Eq. (3) w.r.t. time t, formally:

$$\dot{V}_{OCV}(t) = \dot{V}(t) + \dot{V}_{R_S}(t) + \dot{V}_C(t), \tag{4}$$

where the dot operator denotes the derivative w.r.t. time. Using the equation above the dynamics of the voltage over the RC group and the resistance R_S are:

$$\dot{V}_C(t) = \frac{I(t)}{C} - \frac{V_C(t)}{C \cdot R_P} = \frac{I(t)}{C} - \frac{V_{OCV}(t) - V(t) - R_S \cdot I(t)}{C \cdot R_P}, \tag{5}$$

$$\dot{V}_{R_S}(t) = R_S \cdot \dot{I}(t) + \dot{R}_S \cdot I(t), \tag{6}$$

respectively.

Since this analysis takes into account short periods of time, R_S can be approximated as a constant, *i.e.,* $\dot{R}_S = 0$, as suggested by He et al.

[2] This notation is intended to highlight the dependence of the equivalent parameters from the SoC, SoH, and Temperature (T). From now on, for the sake of simplicity, these dependencies are dropped, i.e., $R_S := R_S(SoC, SoH, T)$, $R_P := R_P(SoC, SoH, T)$, and $C := C(SoC, SoH, T)$.

[3] Notice that the function f may present different characteristics according to the kind of Lithium-ion technology, e.g., the Lithium Ion Phosphate ones. It is known in the literature that the estimation of such batteries using a model-based approach is not a viable option [48], and should be solved with a different approach.

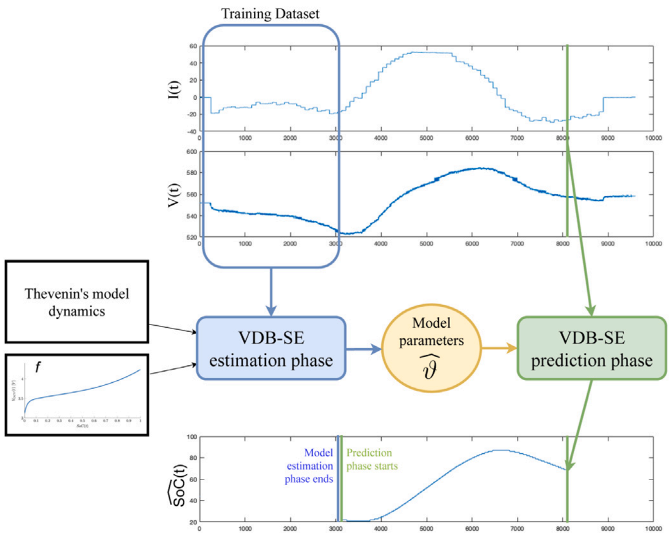

Fig. 3. An example of the algorithm applied to a real signal.

[49]. By combining Eqs. (4), (5), and (6), the final expression of the battery dynamics becomes:

$$\dot{V}(t) - \dot{V}_{OCV}(t) + R_S \cdot \dot{I}(t) + \frac{I(t)}{C} - \frac{V_{OCV}(t) - V(t) - R_S \cdot I(t)}{C \cdot R_P} = 0. \tag{7}$$

Using Eq. (7) and assuming Δt as sampling interval, the battery dynamics equation becomes:

$$\frac{V(t) - V(t-1)}{\Delta t} - \frac{V_{OCV}(t) - V_{OCV}(t-1)}{\Delta t} + R_S \left[\frac{I(t) - I(t-1)}{\Delta t} \right] + \frac{I(t)}{C} - \frac{V_{OCV}(t) - V(t) - R_S \cdot I(t)}{C \cdot R_P} = 0, \tag{8}$$

where backward finite differences had been used to approximate the derivatives.

The VDB-SE algorithm is articulated into two phases, both consistently executed during the operational life of the battery: first, an approximation of the model $\hat{\vartheta}$ of the battery is computed, then, the estimated dynamic of the battery voltage $\hat{V}(\hat{\vartheta}, t)$ derived from the model is used to get an estimate of the SoC $\widehat{SoC}(\hat{\vartheta}, t)$.

A block diagram showing the proposed model is presented in Fig. 3 and an example of execution of the algorithm over time is provided in Fig. 4. In the first phase, VDB-SE estimates a model for the voltage $\hat{V}(\vartheta, t)$ to obtain an approximate value for the Open Circuit Voltage $\hat{V}_{OCV}(\vartheta, t)$. Using a training dataset coming from the time interval $\mathcal{T} := \{\tau, \dots, \tau + N\}$, the VDB-SE algorithm infers a model, which depends on the parameter vector $\vartheta := (R_S, R_P, C, SoC_\tau, Q_{\max})$ which fully characterize Thevenin's approximation of a battery, where SoC_τ denotes the battery SoC at the beginning of the time interval $\mathcal{T}$. Formally, the analytical formalization of this problem is:

$$\min_{\vartheta} \sum_{t=\tau+1}^{\tau+N} |\hat{V}(\vartheta, t) - V(t)|, \tag{9}$$

where the voltage dynamics are denoted by:

$$\hat{V}(\vartheta, t) = \frac{\Delta t \cdot C \cdot R_P}{\Delta t + C \cdot R_P} \left[\left(\frac{1}{\Delta t} \right) \hat{V}(\vartheta, t-1) + \left(\frac{1}{\Delta t} + \frac{1}{C \cdot R_P} \right) \hat{V}_{OCV}(\vartheta, t) - \left(\frac{1}{\Delta t} \right) \hat{V}_{OCV}(\vartheta, t-1) - \left(\frac{R_S}{\Delta t} + \frac{1}{C} + \frac{R_S}{C \cdot R_P} \right) I(t) + \left(\frac{R_S}{\Delta t} \right) \cdot I(t-1) \right], \tag{10}$$

$$\hat{V}_{OCV}(\vartheta, t) = f \left(SoC_\tau + \frac{\Delta t}{3600\, Q_{\max}} \sum_{h=\tau}^{t} I(h) \right), \tag{11}$$

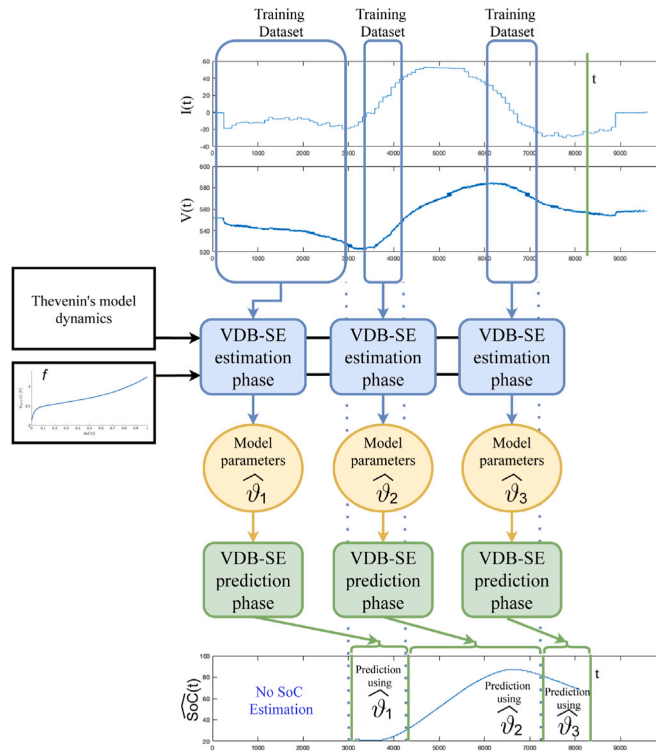

Fig. 4. An example of the VDB-SE over time.

for each $t \in \mathcal{T}$, where Eq. (10) has been derived substituting the voltage and Open Circuit Voltage estimators in Eq. (8), and Eq. (11) uses a CC approach to compute the values of the Open Circuit Voltage. Solving the minimization problem in Eq. (9) requires to set an initial parameter vector $\vartheta^0 := (R_S^0, R_P^0, C^0, SoC_\tau^0, Q_{\max}^0)$, and use an iterative nonlinear optimization procedure to find the optimal vector $\hat{\vartheta} := \left(\hat{R}_S, \hat{R}_P, \hat{C}, \widehat{SoC}_\tau, \hat{Q}_{\max}\right)$.[4]

Subsequently, $\hat{\vartheta}$ is used to generate a prediction of the SoC, $\widehat{SoC}(\hat{\vartheta}, t)$, at time t. More specifically, using the measurements coming from the operational life of the battery $I(t)$ and $V(t)$, the inverse SoC/Open Circuit Voltage relationship $f^{-1}(\cdot)$ and the expression of the Open Circuit Voltage $\hat{V}_{OCV}(\hat{\vartheta}, t)$, the estimated SoC for $t > \tau + N$ becomes $\widehat{SoC}(\hat{\vartheta}, t) = f^{-1}(\hat{V}_{OCV}(\hat{\vartheta}, t))$, where:

$$\hat{V}_{OCV}(\hat{\vartheta}, t) = \frac{\Delta t \cdot \hat{R}_P \cdot \hat{C}}{\Delta t + \hat{R}_P \cdot \hat{C}} \left[\left(\frac{1}{\Delta t} \right) \hat{V}_{OCV}(\hat{\vartheta}, t-1) + \left(\frac{\Delta t + \hat{R}_P \cdot \hat{C}}{\Delta t \cdot \hat{R}_P \cdot \hat{C}} \right) V(t) - \left(\frac{1}{\Delta t} \right) V(t-1) + \left(\frac{\hat{R}_S}{\Delta t} + \frac{1}{\hat{C}} + \frac{\hat{R}_S}{\hat{R}_P \cdot \hat{C}} \right) I(t) - \left(\frac{\hat{R}_S}{\Delta t} \right) I(t-1) \right]. \tag{12}$$

Since the auto-regressive coefficient $\frac{\hat{R}_P \cdot \hat{C}}{\Delta t + \hat{R}_P \cdot \hat{C}}$ in Eq. (12) is smaller than one for any value of $\Delta t > 0$, the estimation process is always stable w.r.t. misspecification of the initial V_{OCV}. This phenomenon will be further investigated in Section 5.2.

Notice that during the operational life of the battery, the above-mentioned phases can be carried out on a moving window of fixed size, so that the resulting estimation is up-to-date w.r.t. the battery status. For instance in Fig. 4, after a first estimation of $\hat{\vartheta}_1$, the VDB-SE algorithm provides a prediction $\widehat{SoC}(\hat{\vartheta}_1, t)$ using such a parameter in Eq. (12). Over time, due to changing environmental conditions or

[4] Each quantity X^0 and $\hat{X}$ denotes the initial and optimal version of the original quantity X, respectively.

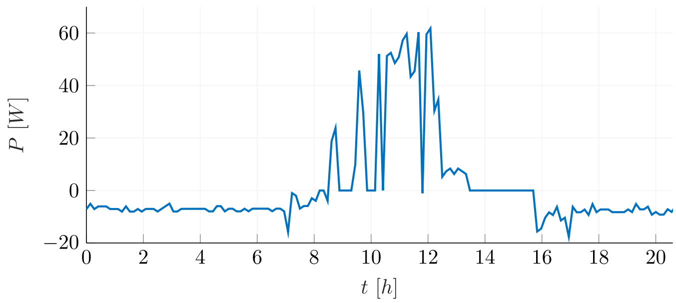

Fig. 5. Power profile input signal for Single-Cell experiments.

Table 2
Characteristics of the simulated cell.

Feature	Value
Rated voltage	3.6 V
Minimum voltage	2.7 V
Maximum voltage	4.2 V
Rated capacity	40 Ah/160 Wh
Rated charging/discharging current	40 A

battery ageing, this model start providing poor performance. To cope with that, a new parameter $\hat{\vartheta}_2$ is estimated on more recent measurements, and the prediction $\widehat{SoC}(\hat{\vartheta}_2, t)$ is performed using the up-to-date model. This process can be repeated every time new data is available.

5. Experiments

In this section, the VDB-SE methodology is tested in two sets of experiments. First, a real self-consumption power profile, provided in Fig. 5, is used to simulate a single battery setting included as energy storage system in a real smart grid. The current $I(t)$ and voltage $V(t)$ time series are generated using this power profile and the corresponding first-order Thevenin's battery model. Notice that the proposed test aims at comparing the performance of the different methods when dealing with biases and different conditions in a fully controlled context, i.e., in which the SoC estimation provided by the methods can be compared with the real value of the SoC.

Second, the real inputs (current and voltage) from a real-world energy storage system are taken into account. The test aims at understanding how VDB-SE performs on the task of estimating the overall SoC of a real battery , given the large number of factors that affect the quality of the estimate on a real system.

5.1. Single-cell experiments

The RC model parameters R_S, R_P, C, and the curve $V_{OCV}(t) = f(SoC(t))$ used for the first experiment are based on the results of a performance test done on a Nickel-Manganese-Cobalt (NMC) cell manufactured by Kokam, model $SLPB100216216H$. Table 2 shows the characteristics of the cell.

The experiments have been performed using a battery simulator developed using real-world battery data, which generates the values of the battery current, voltage and reference SoC over time. This simulator has been implemented in Matlab-Simulink.[5] The code used for the results provided in this section has been run on a Intel(R) I5(R) 8259U @ 2.30 GHz CPU with 8 GB of LPDDR3 system memory. The operating system was macOS 11.2.3, and the experiments have been run on Matlab(R) $R2020b$.

In what follows, the tests conducted use different values of the temperature and SoH set in the simulator. More specifically, the temperatures varies in $T \in \{10\ °\mathrm{C}, 20\ °\mathrm{C}, 30\ °\mathrm{C}\}$, and the SoH varies in $SoH \in \{1, 0.75, 0.5, 0.25, 0\}$, assuming that $p = 0.8$. The tests have been conducted using a real-world power profile, which causes the battery SoC to vary in the range [0.15, 0.9], which includes those SoC values for which the function f is less variable and, therefore, where the SoC estimation task presents the most challenges. Moreover, two types of biases on the current and voltage signals were considered: an offset and a gain bias of 1% for the current, and an offset and gain bias of 0.1% for the voltage, whose magnitudes were chosen so that they are in line with what is provided in the technical data sheet of the measurement instrument [4] used by the battery. In this set of experiments, the two biases are applied to current and voltage simultaneously since, in real life, they might affect the sensors concurrently. These scenario has been denoted from now on with B, while the experiments conducted without any bias has been denoted with WB. Finally, the authors analyse a setting in which the voltage used to estimate the function $f(\cdot)$ is affected by the same offset and gain biases occurring on $V(t)$. This last experiment, from now on referred as BF, exemplifies the case in which the same measuring instrument is used to estimate $f(\cdot)$ and during the operational life of the system.

In the tests, the estimation of the Thevenin's model parameters used in VDB-SE is performed using a sliding window whose width is determined by a variation of the SoC of at least 0.4. More specifically, the estimation phase of VDB-SE is performed each time using the values of current and voltage measurements from a time window $\mathcal{T} = \{\tau, \dots, \tau + N\}$ such that $\max_{t \in \mathcal{T}} SoC(t) - \min_{t \in \mathcal{T}} SoC(t) = 0.4$.[6] In the analysed setting, the cardinality of the time window for the first estimation phase is $N = 43{,}000$, corresponding to approximately 12 h of measurements. The model is used to estimate the Thevenin's model parameters and the initial SoC, and, subsequently, the procedure is repeated on a sliding window with same amplitude as above, each time the SoC variation exceeds 0.2.

During the operational life of the system, the SoC value is propagated using the discrete dynamic equations of the Thevenin's model with the most recent parameter available to estimate the $V_{OCV}(t)$.

The VDB-SE algorithm has been compared with two methods that are suitable in real online applications: the Coulomb Counting (CC) [50] which has a small computational effort, and the model-based method described in Codeca et al. [26], hereafter referred as MB, which works online but requires a priori knowledge of the Thevenin's equivalent model parameters of the battery. Notice that more complex methods from the literature would not constitute a fair comparison to our method since they require the availability of lab experiments to characterize the battery, while VDB-SE only exploits the data coming from the operational life of the battery. The VDB-SE, CC, and MB methods are compared in terms of the percentage error $\epsilon(t)$, defined as follows:

$$\epsilon(t) = 100 \left| SoC(t) - \widehat{SoC}(\hat{\vartheta}, t) \right|.$$

Results. A preliminary experiment has been conducted to evaluate the capabilities of VDB-SE in the case no noise and bias are present. The implemented approach, applied to a batch of 20,000 noiseless measurements generated from a stationary battery, *e.g.*, with fixed temperature and SoH and with no measurement biases, can reconstruct the dynamics of the voltage $V(t)$ with an average error of 10^{-2} V and a corresponding error on the SoC estimation of $\epsilon(t) \leq 0.01\%$.

[5] https://it.mathworks.com/products/simulink.html. The corresponding code, and the code to replicate the experiments of this section are available at https://github.com/marcomussi/vdbse.

[6] In generic settings, it is possible to set a percentage of the SoC to determine the length of the period N used for optimizing the model parameters, to use a fixed number of samples, or use a condition on both the variation of the SoC percentage and a maximum number of samples.

Table 3
Errors (percentage) on the different setting as the SoH, temperature and different biases are present on the battery measurements.

SoH	T	WB			B			BF		
		CC	VDB-SE	MB	CC	VDB-SE	MB	CC	VDB-SE	MB
1	10 °C	0.00	0.15	0.00	0.94	1.32	1.31	0.94	0.22	0.04
	20 °C	0.00	0.07	0.00	0.94	1.28	1.29	0.94	0.14	0.02
	30 °C	0.00	0.01	0.07	0.94	1.28	1.29	0.94	0.14	0.06
0.75	10 °C	0.90	0.17	0.01	1.17	1.32	1.31	1.17	0.24	0.05
	20 °C	0.91	0.07	0.01	1.18	1.28	1.29	1.18	0.15	0.03
	30 °C	0.91	0.01	0.05	1.18	1.28	1.29	1.18	0.15	0.05
0.5	10 °C	1.91	0.19	0.02	2.15	1.31	1.30	2.15	0.26	0.06
	20 °C	1.92	0.06	0.02	2.16	1.27	1.28	2.16	0.15	0.04
	30 °C	1.93	0.01	0.05	2.17	1.27	1.28	2.17	0.15	0.04
0.25	10 °C	3.03	0.20	0.04	3.26	1.31	1.29	3.26	0.27	0.07
	20 °C	3.05	0.07	0.04	3.29	1.27	1.28	3.29	0.16	0.05
	30 °C	3.06	0.02	0.04	3.29	1.27	1.28	3.29	0.16	0.04
0	10 °C	4.29	0.20	0.05	4.52	1.30	1.29	4.52	0.26	0.09
	20 °C	4.32	0.07	0.05	4.55	1.26	1.27	4.55	0.17	0.07
	30 °C	4.34	0.02	0.03	4.57	1.26	1.27	4.57	0.16	0.03

Table 3 shows the results of the experimental campaign conducted on synthetic data. First, variations of the operational temperature do not change significantly (less than 0.07%) the estimation error of the CC and MB methods, while generally higher values of the temperature provide smaller errors for VDB-SE, with a decrease in the range [0.0%, 0.18%]. Instead, regarding variations of the SoH, MB and VDB-SE deals with a degradation of the battery health, with an error increasing of at most of 0.05% from $SoH = 1$ to $SoH = 0$. Conversely, the CC methods has a significant increase in terms of error, *i.e.,* from 0%–1% for $SoH = 1$ to 4.3%–4.7% for $SoH = 0$. More specifically, MB maintains an almost constant estimation error over different SoHs, thanks to the closed-loop approach, which allows to adapt to the new battery behaviour. Similarly, VDB-SE does not suffer from an increased error due to SoH variations since its optimization procedure adapts the value of $Q_{\max}$. Both algorithms keep the error below 1.32%, where CC error increases up to 4.5% as the battery status worsen. Finally, comparing the B and BF settings, notice that the coherence in terms of measurements when estimating the $f(\cdot)$ relationship and the values of the current and voltage from the battery, allows VDB-SE and MB to recover from the introduced biases. Conversely, CC does still have an error magnified by the introduction of current and voltage biases.

Most of the times MB and VDB-SE provide similar error, *i.e,* around 0.2% in the WB and BF cases, and around 1.3% in the B case. Moreover, their difference in terms of performance is always smaller than 0.2%. This highlight the capability of VDB-SE to provide a good SoC estimation, even if it does not require a priori knowledge of the parameters of the Thevenin's equivalent model. Conversely, MB is providing good estimates but only correctly setting the Thevenin's model parameters at the beginning of the estimation procedure.

The predictions over time of VDB-SE and the comparison methods in the settings B and BF are presented in Fig. 6. VDB-SE presents an estimate of the SoC that is qualitatively better than the CC and comparable with MB, preventing the estimate from diverging from the real SoC over time.

Fig. 6a represents the error $\epsilon(t)$ for the analysed methods in the presence of the offset and gain biases for both current and voltage, as usually happens in real systems. The figure shows how CC has no mechanism to avoid the ever-increasing estimation error. Conversely, MB can recover from the occurrence of a large estimation error as it exceeds a predetermined threshold. This phenomenon is due to the correction mechanism provided by the closed-loop structure, used by MB, which evaluates the battery voltage, and introduces a correction if the predicted and actual voltage values differ more than a predefined threshold. In this experiment, VDB-SE provides an estimation that is qualitative comparable with MB. Indeed, the VDB-SE model prevents divergence between estimated and real SoC and keeps the error $\epsilon(t)$ strictly below 2% of the SoC range on average on the samples $\{\tau + N, \dots, T\}$, *i.e.,* after the first optimization phase.

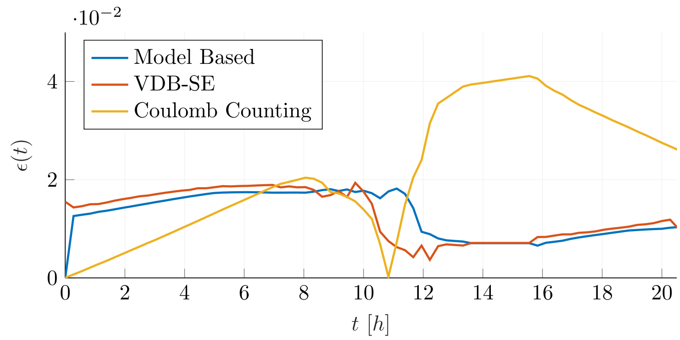

(a) Function $f(\cdot)$ estimated with a different measuring instrument.

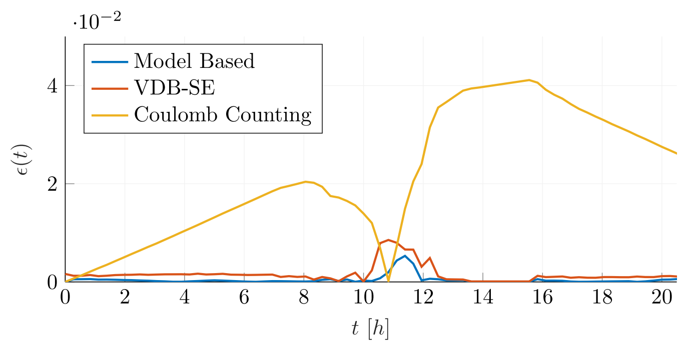

(b) Function $f(\cdot)$ estimated with the same instrument.

Fig. 6. Error in SoC estimation in presence of measurement biases in case of State of Health equal to 0.5.

Fig. 6b shows a test to evaluate the performance in the case where $f(\cdot)$ is estimated using the same measuring instrument of the test. In this figure, CC behaves, as in previous experiments, as the voltage measurement bias does not affect its performance. Conversely, MB and VDB-SE provide smaller errors (less than 1%) than those present in the previous cases, even if the voltage and current biases are present with the same magnitude as before. More in detail, the performance of VDB-SE is considerably better than the one in Fig. 6a because, being the two biases equal, their influences cancel each other out in the estimation process. This suggests that VDB-SE should be run with the same measuring instruments used for the $f(\cdot)$ estimation to provide better estimation performance.

In summary, VDB-SE is the only algorithm capable, among those investigated, to deal (without preliminary information about the system) with both the offset and gain biases commonly found on real-world sensors and, therefore, represents a viable option on real-world systems.

5.2. Field experiments

The second experiment evaluates the performance of the VDB-SE algorithm on a real battery storage system installed at the Test Facility of RSE in Milan (see Sandroni et al. [51] for details). Typically, this kind of system is used to improve the flexibility of the smart grid, enabling better exploitation of the installed renewable resources and providing grid services to the main grid. The system consists of a rack of nine lithium-ion modules of 3.55 kWh each, connected in series for total energy of 32 kWh. An additional module is dedicated to the protection and management of the cells. Every module has 16 Lithium-Manganese-Oxide (LMO) cells manufactured by SAMSUNG with a capacity of 60 Ah. The main characteristics of the battery are listed in Table 4. Notice that the complexity of the system is still

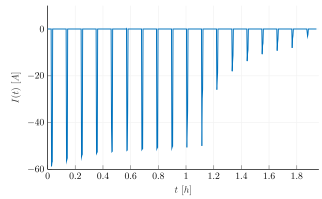

(a) Current signal used to define the $f(\cdot)$ relationship in the Field Experiments.

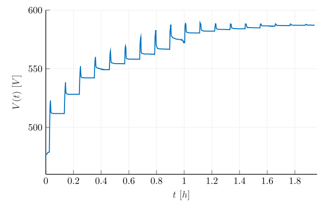

(b) Voltage signal used to define the $f(\cdot)$ relationship in the Field Experiments.

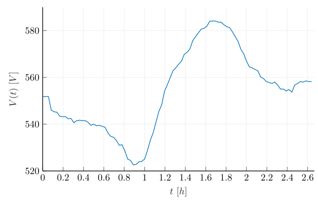

(c) Voltage test input signal for the Field Experiments.

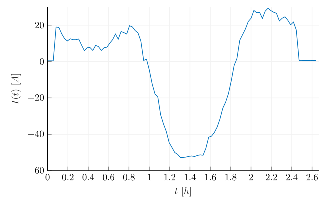

(d) Current test input signal for the Field Experiments.

Fig. 7. Data used for in the real battery storage system experiment.

Table 4
Characteristics of the real-world battery.

Feature	Value
Rated voltage	532.8 V
Minimum voltage	432.0 V
Maximum voltage	593.3 V
Rated capacity	60 Ah/32 kWh
Number of cells	144
Rated charging/discharging power	32 kW

captured by a single Thevenin's model, and no information on the cell structure, neither their connection scheme, are needed for the VDB-SE modelling approach.

The function $f(\cdot)$ that characterizes the relationship between SoC and V_{OCV}, and the value of $Q_{\max}$ of the battery rack were inferred with a laboratory test, in a way comparable the one described in Section 5.1. The data used to estimate $f(\cdot)$ are provided in Fig. 7a (current) and Fig. 7b (voltage). The SoC estimation test was performed on a real smart grid load profile of about 3 hours of current and voltage sampled at 1 Hz presented in Figs. 7c–7d. The reference value of the SoC is determined through CC that, as pointed out before, has a small cumulative error over short time periods. The value of $Q_{\max}$ used by CC has been estimated using an offline discharge test. The MB model was not applied here, since the information required to properly set its hyperparameter were not available. As in the previous cases, the model estimation is performed using a sliding window that includes 0.4 of the SoC range, and the model update is performed as soon as a variation of 0.2 of the SoC occurs.

Finally, the stability of the VDB-SE algorithm is tested in a setting in which the stream of measurements is discontinued for a certain amount of time during which the model of the battery is assumed to be constant. This behaviour is simulated providing at time $t = 6000$, during the prediction phase of VDB-SE, and after the estimation phase, a misspecified value of $\widehat{SoC}(\hat{\vartheta}, t)$ and, hence $\hat{V}_{OCV}(\hat{\vartheta}, t)$.

More specifically, the experiments have been conducted using values $\widehat{SoC}(\hat{\vartheta}, k) \in \{0.1, 0.2, \dots, 1\}$ for the value of the SoC at the initial time instant $k > \tau + N$, where the true value of the initial SoC is $SoC(t) = 0.4$.

Results. Fig. 8a shows the actual and estimated SoC value provided by VDB-SE and Fig. 8b shows the corresponding SoC estimation error $\epsilon(t)$. Overall the VDB-SE algorithm provides a good approximation of the SoC, with an average error over the test set of less than 2.1%. The fact that the dataset has a current $I(t) > 0$ when the voltage is constant

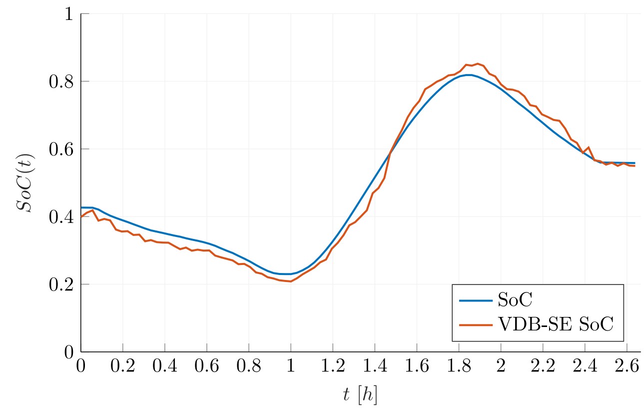

(a) Real SoC and VDB-SE estimation on real data.

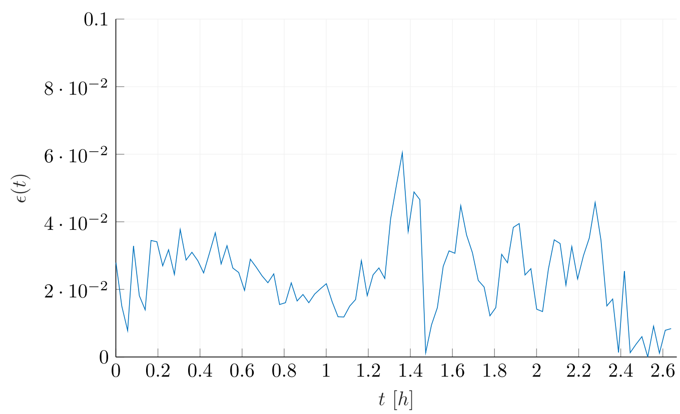

(b) VDB-SE error $\epsilon(t)$ on real data.

Fig. 8. Results for the experiment on real data.

suggests the presence of an offset bias on the current input. Therefore, even in this case, VDB-SE handles biases in the measurements, preventing the divergence of the SoC estimate from the real one (or converge to a good approximation of the SoC value in case of divergence due to interruption of the signals). This test also shows how the VDB-SE algorithm can handle complex energy storage systems, even without knowing their structure.

The time required to execute VDB-SE over the set of data considered for this experiment on the device described above is on average lower than 3 s. Indeed, the first training phase requires approximately 0.5 s and a single prediction requires $2 \cdot 10^{-7}$ s.[7]

Fig. 9a reports the estimation provided by VDB-SE as the values of $\widehat{SoC}(\hat{\vartheta}, k)$ varies, and Fig. 9b presents the corresponding errors $\epsilon(t)$. The figure shows only the first 1500 time steps since the effects of the misspecification of the initial SoC fades completely after such a period for all the values of the initial SoC $\widehat{SoC}(\hat{\vartheta}, k)$ analysed. More specifically, the errors decrease below 5% after ≈ 1000 time steps and converges to the one provided by the VDB-SE without misspecification of the SoC before the end of the analysed period. As expected, the time required for the convergence is slower if the initial misspecification error is more evident, while for small errors, *e.g.*, for $\widehat{SoC}(\hat{\vartheta}, k) = 0.4$, the estimation error decreases faster.

6. Conclusions and future works

The problem of estimating the SoC of lithium-ion batteries is of paramount importance in energy management systems. Indeed, they

[7] The time required to provide a prediction by the CC and MB methods is comparable with the one used by VDB-SE.

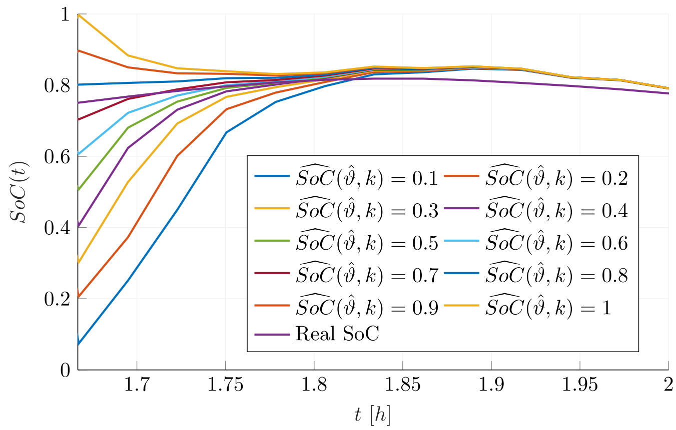

(a) $SoC(t)$ estimation.

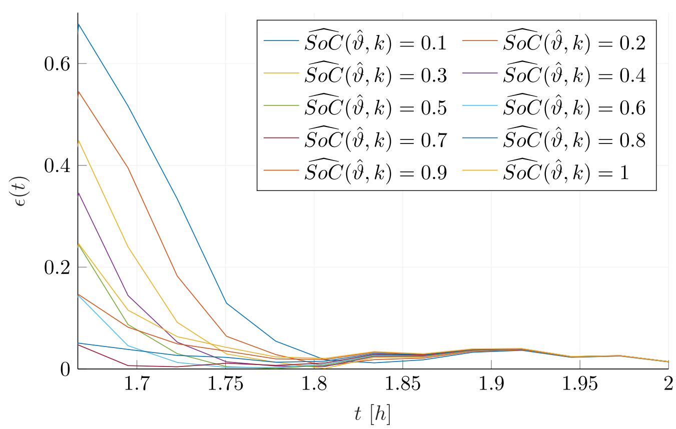

(b) Error ϵ(t).

Fig. 9. Results for the experiment on real data in presence of different wrong SoC starting values. The numbers in the legends denotes intensity of the misspecification of the initial SoC.

constitute reliable and cheap energy storage devices, and an accurate estimate of their residual capacity allows fine-grained control of the overall system. In this paper, a novel algorithm, namely VDB-SE, has been presented. This method exploits the mathematical characterization of the battery offered by Thevenin's model to define a specifically crafted optimization problem for the SoC estimation problem. Thanks to this modelling approach, it is possible to estimate the equivalent battery parameters and use them to predict the SoC during its operational life without requiring *a priori* characteristics of the storage system and avoiding its periodic recalibration. These characteristics make VDB-SE a candidate for articulated storage systems, such as smart grids and automotive applications, thanks to its ability to exploit only the measurements coming from the battery and not requiring preliminary tests on the storage device. Experimental results on both synthetically generated and real-world data showed that the VDB-SE algorithm attains high performance in the SoC estimation under various sets of conditions. Specifically, it showed less than 0.2% degradation in the error over the synthetic experiments w.r.t. MB, a model that requires a priori information on the battery to properly function, and an average error of less than 2.1% over the SoC estimation of a real energy storage system. The same experiments showed that the proposed algorithm can handle changes in the temperature, degradation of the battery, and measurement biases.

Future works will consider the analysis of the battery State of Health, to reshape what is proposed here, focusing on the estimate of the internal resistance and its behaviour w.r.t. degradation and the effect of the temperature over time, in addition to the evolution of the maximum capacity during the ageing process. Furthermore, an interesting study is the evaluation of the impact of VDB-SE algorithm when integrated into microgrid controllers.

Nomenclature

The symbols used in the paper are:

t	Time instant
$SoC(t)$	State of Charge at time instant t
$Q(t)$	Battery capacity at time instant t
$Q_{max}(t)$	Maximum capacity of the battery at time instant t
$SoH(t)$	State of Health at time instant t
p	Rate of the nominal capacity for which the battery cannot be used anymore
Q_N	Battery nominal capacity
R_S	Internal resistance
R_P	Polarization resistance
C	Battery capacitance
$V_{OCV}(t)$	Voltage over the OCV source
$I(t)$	Current signal measured from the battery
$V(t)$	Voltage signal measured over the battery
$f(\cdot)$	Function providing the $V_{OCV}(t)$ given the current $SoC(t)$
$\mathcal{T}$	Set of the time instant used in estimation phase
$V_C(t)$	Voltage over the RC group
$V_{R_S}(t)$	Voltage over the internal resistor
$\dot{V}_{OCV}(t)$	Derivative over time of $V_{OCV}(t)$
$\dot{V}(t)$	Derivative over time of $V(t)$
$\dot{V}_{R_S}(t)$	Derivative over time of $V_{R_S}(t)$
$\dot{V}_C(t)$	Derivative over time of $V_C(t)$
$\dot{I}(t)$	Derivative over time of $I(t)$
$\dot{R}_S$	Derivative over time of R_S
T	Temperature
Δt	Sampling interval
ϑ	Vector parameters of the Thevenin's battery model
$\widehat{SoC}(\hat{\vartheta},t)$	Estimates of the SoC at time instant t
$\hat{V}(\hat{\vartheta},t)$	Estimates of the voltage $V(t)$ at time instant t
$\hat{V}_{OCV}(\hat{\vartheta},t)$	Estimates of the Open Circuit Voltage $V_{OCV}(t)$ at time instant t
τ	Starting time for the estimation phase
N	Estimation phase length
SoC_τ	Battery SoC at the beginning of the time interval $\mathcal{T}$
ϑ^0	Initial parameter vector
$\hat{\vartheta}$	Estimated optimal parameter vector
$\epsilon(t)$	SoC estimation error at time instant t

The acronym used in the paper are:

$VDB-SE$	Voltage Dynamic-Based State Estimation
SoC	State of Charge
SoH	State of Health
CC	Coulomb Counting
MB	Model Based
ANN	Artificial Neural Networks
SVM	Support Vector Machines
KF	Kalman Filter
EKF	Extended Kalman Filter
$AEKF$	Adaptive Extended Kalman Filter
UKF	Unscented Kalman Filter
OCV	Open Circuit Voltage
B	Experiments with measurement Bias
WB	Experiments Without measurement Bias
BF	Experiments where the $f(\cdot)$ function is affected by the same bias as the voltage and current measurements

CRediT authorship contribution statement

Marco Mussi: Methodology, Software, Validation, Data curation, Visualization. **Luigi Pellegrino:** Investigation, Resources, Supervision. **Marcello Restelli:** Conceptualization, Supervision, Writing – review & editing. **Francesco Trovò:** Methodology, Formal analysis, Writing – original draft.

Declaration of competing interest

The authors declare that they have no known competing financial interests or personal relationships that could have appeared to influence the work reported in this paper.

Acknowledgement

Founding: This work has been financed by the Research Fund for the Italian Electrical System in compliance with the Decree of Minister of Economic Development April 16, 2018.

References

[1] A. Mey, P. Hutchins, V. Linga, Battery Storage in the United States: An Update on Market Trends, second ed., EIA, Washington DC, 2020.
[2] P. Ralon, M. Taylor, A. Ilas, H. Diaz-Bone, K. Kairies, Electricity storage and renewables: Costs and markets to 2030, International Renewable Energy Agency, Abu Dhabi, UAE, 2017.
[3] B. Diouf, R. Pode, Potential of lithium-ion batteries in renewable energy, Renew. Energy 76 (2015) 375–380.
[4] National Instruments, Datasheet NI 9201, 2016.
[5] A. Ausswamaykin, B. Plangklang, Design of real time battery management unit for PV-hybrid system by application of coulomb counting method, Energy Power Eng. 2014 (2014).
[6] W. Waag, C. Fleischer, D.U. Sauer, Critical review of the methods for monitoring of lithium-ion batteries in electric and hybrid vehicles, J. Power Sources 258 (2014) 321–339.
[7] X. Ding, D. Zhang, J. Cheng, B. Wang, P.C.K. Luk, An improved thevenin model of lithium-ion battery with high accuracy for electric vehicles, Appl. Energy 254 (2019) 113615.
[8] Z.M. Salameh, M.A. Casacca, W.A. Lynch, A mathematical model for lead-acid batteries, IEEE Trans. Energy Convers. 7 (1) (1992) 93–98.
[9] M. Zhang, X. Fan, Review on the state of charge estimation methods for electric vehicle battery, World Electr. Veh. J. 11 (1) (2020) 23.
[10] M.H. Lipu, M. Hannan, A. Hussain, A. Ayob, M.H. Saad, T.F. Karim, D.N. How, Data-driven state of charge estimation of lithium-ion batteries: Algorithms, implementation factors, limitations and future trends, J. Cleaner Prod. (2020) 124110.
[11] M.O. Qays, Y. Buswig, M.L. Hossain, A. Abu-Siada, Recent progress and future trends on state of charge estimation methods to improve battery-storage efficiency: A review, CSEE J. Power Energy Syst. (2020).
[12] K.S. Ng, C.-S. Moo, Y.-P. Chen, Y.-C. Hsieh, Enhanced coulomb counting method for estimating state-of-charge and state-of-health of lithium-ion batteries, Appl. Energy 86 (9) (2009) 1506–1511.
[13] W. Shen, C. Chan, E. Lo, K. Chau, A new battery available capacity indicator for electric vehicles using neural network, Energy Convers. Manage. 43 (6) (2002) 817–826.
[14] W. Shen, K. Chau, C.C. Chan, E.W. Lo, Neural network-based residual capacity indicator for nickel-metal hydride batteries in electric vehicles, IEEE Trans. Veh. Technol. 54 (5) (2005) 1705–1712.
[15] L. Kang, X. Zhao, J. Ma, A new neural network model for the state-of-charge estimation in the battery degradation process, Appl. Energy 121 (2014) 20–27.
[16] T. Weigert, Q. Tian, K. Lian, State-of-charge prediction of batteries and battery–supercapacitor hybrids using artificial neural networks, J. Power Sources 196 (8) (2011) 4061–4066.
[17] J. Tian, R. Xiong, W. Shen, J. Lu, State-of-charge estimation of LiFePO4 batteries in electric vehicles: A deep-learning enabled approach, Appl. Energy 291 (2021) 116812.
[18] Y. Guo, Z. Yang, K. Liu, Y. Zhang, W. Feng, A compact and optimized neural network approach for battery state-of-charge estimation of energy storage system, Energy 219 (2021) 119529.
[19] J.C.A. Anton, P.J.G. Nieto, C.B. Viejo, J.A.V. Vilán, Support vector machines used to estimate the battery state of charge, IEEE Trans. Power Electron. 28 (12) (2013) 5919–5926.
[20] J.A. Antón, P.G. Nieto, F. de Cos Juez, F.S. Lasheras, M.G. Vega, M.R. Gutiérrez, Battery state-of-charge estimator using the SVM technique, Appl. Math. Model. 37 (9) (2013) 6244–6253.
[21] T. Hansen, C.-J. Wang, Support vector based battery state of charge estimator, J. Power Sources 141 (2) (2005) 351–358.
[22] S. Malkhandi, Fuzzy logic-based learning system and estimation of state-of-charge of lead-acid battery, Eng. Appl. Artif. Intell. 19 (5) (2006) 479–485.
[23] A.J. Salkind, C. Fennie, P. Singh, T. Atwater, D.E. Reisner, Determination of state-of-charge and state-of-health of batteries by fuzzy logic methodology, J. Power Sources 80 (1–2) (1999) 293–300.
[24] X. Hu, S. Li, H. Peng, A comparative study of equivalent circuit models for li-ion batteries, J. Power Sources 198 (2012) 359–367.
[25] M. Einhorn, V. Conte, C. Kral, J. Fleig, Comparison of electrical battery models using a numerically optimized parameterization method, in: 2011 IEEE Vehicle Power and Propulsion Conference, IEEE, 2011, pp. 1–7.
[26] F. Codeca, S.M. Savaresi, G. Rizzoni, On battery state of charge estimation: A new mixed algorithm, in: IEEE International Conference on Control Applications, IEEE, 2008, pp. 102–107.
[27] S. Boulmrharj, R. Ouladsine, Y. NaitMalek, M. Bakhouya, K. Zine-dine, M. Khaidar, M. Siniti, Online battery state-of-charge estimation methods in micro-grid systems, J. Energy Storage 30 (2020) 101518.
[28] R.E. Kalman, A new approach to linear filtering and prediction problems, J. Basic Eng. 82 (1960) 35–45.
[29] G. Welch, G. Bishop, An introduction to the Kalman filter, Technical Report, University of North Carolina at Chapel Hill, Department of Computer Science, 1995.
[30] S.J. Julier, J.K. Uhlmann, New extension of the Kalman filter to nonlinear systems, in: Signal Processing, Sensor Fusion, and Target Recognition VI, Vol. 3068, International Society for Optics and Photonics, 1997, pp. 182–193.
[31] G.L. Plett, Extended Kalman filtering for battery management systems of LiPB-based HEV battery packs: Part 2. Modeling and identification, J. Power Sources 134 (2) (2004) 262–276.
[32] G.L. Plett, Extended Kalman filtering for battery management systems of LiPB-based HEV battery packs: Part 3. State and parameter estimation, J. Power Sources 134 (2) (2004) 277–292.
[33] A. Vasebi, S. Bathaee, M. Partovibakhsh, Predicting state of charge of lead-acid batteries for hybrid electric vehicles by extended Kalman filter, Energy Convers. Manage. 49 (1) (2008) 75–82.
[34] R. Xiong, H. He, F. Sun, K. Zhao, Evaluation on state of charge estimation of batteries with adaptive extended Kalman filter by experiment approach, IEEE Trans. Veh. Technol. 62 (1) (2012) 108–117.
[35] H. He, R. Xiong, X. Zhang, F. Sun, J. Fan, State-of-charge estimation of the lithium-ion battery using an adaptive extended Kalman filter based on an improved Thevenin model, IEEE Trans. Veh. Technol. 60 (4) (2011) 1461–1469.
[36] W. Xu, S. Wang, C. Jiang, C. Fernandez, C. Yu, Y. Fan, W. Cao, A novel adaptive dual extended Kalman filtering algorithm for the Li-ion battery state of charge and state of health co-estimation, Int. J. Energy Res. (2021).
[37] R. Mehra, On the identification of variances and adaptive Kalman filtering, IEEE Trans. Automat. Control 15 (2) (1970) 175–184.
[38] F. Sun, X. Hu, Y. Zou, S. Li, Adaptive unscented Kalman filtering for state of charge estimation of a lithium-ion battery for electric vehicles, Energy 36 (5) (2011) 3531–3540.
[39] S.-L. Wang, C.-M. Yu, C. Fernandez, M.-J. Chen, G.-L. Li, X.-H. Liu, Adaptive state-of-charge estimation method for an aeronautical lithium-ion battery pack based on a reduced particle-unscented kalman filter, J. Power Electron. 18 (4) (2018) 1127–1139.
[40] S. Wang, C. Fernandez, C. Yu, Y. Fan, W. Cao, D.-I. Stroe, A novel charged state prediction method of the lithium ion battery packs based on the composite equivalent modeling and improved splice Kalman filtering algorithm, J. Power Sources 471 (2020) 228450.
[41] W. Cao, S.-L. Wang, C. Fernandez, C.-Y. Zou, C.-M. Yu, X.-X. Li, A novel adaptive state of charge estimation method of full life cycling lithium-ion batteries based on the multiple parameter optimization, Energy Sci. Eng. 7 (5) (2019) 1544–1556.
[42] B. Li, S. Wang, C. Fernandez, C. Yu, L. Xia, Y. Fan, A linear recursive state of power estimation method based on fusion model of voltage and state of charge limitations, J. Energy Storage 40 (2021) 102583.
[43] W. He, N. Williard, C. Chen, M. Pecht, State of charge estimation for li-ion batteries using neural network modeling and unscented Kalman filter-based error cancellation, Int. J. Electr. Power Energy Syst. 62 (2014) 783–791.
[44] J.P. Rivera-Barrera, N. Muñoz Galeano, H.O. Sarmiento-Maldonado, Soc estimation for lithium-ion batteries: Review and future challenges, Electronics 6 (4) (2017) 102.
[45] M. Berecibar, I. Gandiaga, I. Villarreal, N. Omar, J. Van Mierlo, P. Van den Bossche, Critical review of state of health estimation methods of Li-ion batteries for real applications, Renew. Sustain. Energy Rev. 56 (2016) 572–587.
[46] Q.-Q. Yu, R. Xiong, L.-Y. Wang, C. Lin, A comparative study on open circuit voltage models for lithium-ion batteries, Chin. J. Mech. Eng. 31 (1) (2018) 65.

[47] C. Zhang, J. Jiang, L. Zhang, S. Liu, L. Wang, P.C. Loh, A generalized SOC-OCV model for lithium-ion batteries and the SOC estimation for LNMCO battery, Energies 9 (11) (2016) 900.

[48] L. Xu, J. Wang, Q. Chen, Kalman filtering state of charge estimation for battery management system based on a stochastic fuzzy neural network battery model, Energy Convers. Manage. 53 (1) (2012) 33–39.

[49] H. He, R. Xiong, H. Guo, Online estimation of model parameters and state-of-charge of LiFePO4 batteries in electric vehicles, Appl. Energy 89 (1) (2012) 413–420.

[50] I. Baccouche, A. Mlayah, S. Jemmali, B. Manai, N.E.B. Amara, Implementation of a Coulomb counting algorithm for SOC estimation of li-ion battery for multimedia applications, in: IEEE International Multi-Conference on Systems, Signals & Devices (SSD), IEEE, 2015, pp. 1–6.

[51] C. Sandroni, M. Verga, R. Lazzari, M. Fantini, M. Sacchi, V. Prandoni, Rse's microgrid: A facility for research, development and testing of future distributed generation and microgrid technologies, in: AEIT International Annual Conference (AEIT), 2016, pp. 1–6.